# **ORGANOMETALLICS**

pubs.acs.org/Organometallics Article

# Improved Trianionic Pincer Ligand Synthesis for Cyclic Polymer Catalysts

Vineet K. Jakhar, Yu-Hsuan Shen, Sung-Min Hyun, Alec M. Esper, Ion Ghiviriga, Khalil A. Abboud, Daniel W. Lester, and Adam S. Veige\*



Cite This: Organometallics 2023, 42, 1339–1346



ACCESS I

Metrics & More

Article Recommendations

Supporting Information

**ABSTRACT:** An easier, safer, and scalable approach to the synthesis of a trianionic pincer ligand and its use in the preparation of the Mo cyclic polymer catalyst  $[O_2C((p-OMe-C_6H_4)C=)Mo(\eta^2-CH\equiv C^tBu)(THF)]$  (7) are reported. The synthesis of the  $[^tBuOCO]Me_2$  (1) ligand is simplified to a reaction that allows scaling up, thus reducing the main barrier to accessing cyclic polymer catalysts. The synthesis allows for the derivatization of the  $C_{ipso}$  carbon of the central ring of the pincer. Taking advantage of this, a deuterium atom was substituted for kinetic isotope measurements. Complex 7 was tested for activity in the polymerization of phenylacetylene. Confirmation of the cyclic polymer topology comes from gel permeation chromatography (GPC), dynamic light scattering (DLS), and intrinsic viscosity  $(\eta)$  measurements.



### INTRODUCTION

Manipulating the dispersity (D), branching density and main chain composition, molecular weight  $(M_w)$ , and repeat units in polymers imparts many functional properties of macromolecules. The polymer chain ends are an important feature that determines both solution and solid-state polymer properties. Removing chain ends to create cyclic polymers opens an "endless" opportunity to alter polymer composition, and therefore their application diversity. Prolonging blood circulation<sup>3,4</sup> and improving drug delivery<sup>4,5</sup> using cyclic polymers are two applications enabled by a lack of chain ends. On surfaces, cyclic polymers exhibit lower surface friction, 6-8 antifouling capability, 8 and improved dewetting kinetics during annealing.9 Unique solution phase improvements over linear polymers include lower intrinsic viscosities, 10 increased micelle cloud point temperatures, 11 and higher refractive indices. 12,13

Tailored transition metal catalysts featuring a tethered metal—carbon multiple bond, or in one case a metal-lacyclobutane, <sup>14</sup> are initiators for ring expansion metathesis polymerization (REMP). <sup>14–21</sup> Cyclic alkenes, most commonly norbornene, <sup>15–17,19</sup> undergo ring expansion with tethered-metal carbon double bonds to give cyclic polymers. REMP of cyclic alkenes provides cyclic polymers <sup>22</sup> with stereoregular chains, <sup>15–17</sup> bottlebrushes, <sup>23,24</sup> gels, <sup>23,25</sup> and/or cross-linked networks. <sup>25</sup> In a mechanism yet to be examined in depth, transition metal complexes can also polymerize alkynes to obtain cyclic polymers. <sup>26</sup> Key to these recent advances is the synthesis of new catalysts with tailorable ligands. Often ligand synthesis is the limiting step in the overall atom economics of catalyst design and ultimate polymerization efficiency tabu-

lation. In this work, significant improvement in ligand synthesis is realized.

The methyl-protected precursor ['BuOCO]Me<sub>2</sub> (1) and the demethylated ligand ['BuOCO]H<sub>2</sub> (2)<sup>27,28</sup> employed in REMP catalyst synthesis is a multistep sequence that requires 'BuLi and a Pd-catalyzed coupling reaction. *o*-Bromination, methyl-protection, a Pd-catalyzed cross-coupling reaction (Negishi coupling), and finally deprotection yield the functional ligand (Scheme 1).<sup>28</sup> Although Pd-catalyzed cross-

Scheme 1. Previously Reported Synthesis of Trianionic Pincer Proligand ['BuOCO]H<sub>2</sub> (2)

Special Issue: Early Transition Metals in Organometallic Chemistry

Received: January 27, 2023 Published: March 29, 2023





coupling is a popular method to form  $C(sp^2)-C(sp^2)$  bonds due to its versatility, the use of 'BuLi limits efficiency during lithiation. Lithiation of 2-bromo-6-tert-butylanisole using 'BuLi is temperature sensitive due to an undesired elimination reaction of tert-butyl bromide in the presence of a strong base. Furthermore, scaling the reaction makes heat dissipation harder, leading to local heat accumulation.

Here, we present a new ligand synthesis that utilizes "BuLi, circumvents the Pd coupling reaction, and is scalable. Synthesized using proligand 2 is a Mo-REMP catalyst that initiates the polymerization of phenylacetylene to yield cyclic polymers. In addition, variable temperature NMR spectroscopy, a deuterium labeling study, and DFT calculations provide evidence of an unusual fluxional ligand dynamic.

### RESULTS AND DISCUSSION

Hart and co-workers developed the synthesis of *m*-terphenyls through successive nucleophilic displacements of 1,2,3-trihalobenzene with excess Grignard reagents in 1991.<sup>29</sup> Five years after, they carried out the same synthesis using aryl lithium and 1,3-dichlorobenzene rather than Grignard and trihalobenzene substrates (Scheme 2a).<sup>30</sup> Adapting the Hart protocol provides a convenient and scalable synthesis of ['BuOCO]Me<sub>2</sub> (1) (Scheme 2b).

Scheme 2. (a) *m*-Terphenyl Syntheses via Successive Nucleophilic Displacement Developed by Hart and Coworkers Using 1,2,3-Trihalobenzene and Grignard Reagents; (b) Adapted Synthesis of ['BuOCO]Me<sub>2</sub> (1)

Adding 1.5 equiv of 2.5 M "BuLi in hexanes to a solution of 2-bromo-6-tert-butylanisole in diethyl ether at -10 °C (in a cooling bath of ice and NaCl) followed by stirring for 1 h yields 3-tert-butyl-2-methoxyphenyl lithium. Slow addition (20 min) of 1,3-dichlorobenzene to the 3-tert-butyl-2-methoxyphenyl lithium slurry and stirring the reaction mixture overnight followed by acidic workup yields ['BuOCO]Me<sub>2</sub> (1). Recrystallization of the crude mixture in cold isopropanol (-5 °C) affords yellow 1 in 25% yield. Since 2-tert-butylanisole (liquid) and 1 are miscible, isolation via recrystallization was low yielding, compared to the % conversion measured by ¹H NMR spectroscopy (50–60%). The reaction is scalable and an attempt with 190 g (0.79 mol) of 2-bromo-6-tert-butylanisole yielded 48.3 g (0.12 mol, 30%) of 1.

Despite the low isolated yield, this new synthetic method has several advantages over the previously reported Pd catalyzed coupling reaction:

- 1. Considering its high pyrophoricity, substitution of <sup>t</sup>BuLi with <sup>n</sup>BuLi enhances safety. <sup>31,32</sup>
- The lithiation step is more reliable on a large scale with no eliminating side reaction of 'BuBr and ArLi above -78 °C.
- 3. Cost savings come from avoiding a Pd-catalyzed coupling reaction and switching the substrate from 1,3-dibromobenzene (100 g, \$188) to 1,3-dichlorobenzene (100 g, \$16).
- 4. The new synthetic method permits the functionalization of the *ipso* carbon by simply changing the quenching agent. For example, quenching the reaction with  $D_2O$  provides the deuterated [ ${}^tBuOCDO$ ]Me<sub>2</sub> (1- $d_1$ ) product, used below to study kinetic isotope effects (KIE).

Treating the proligand [ ${}^tBuOCO]H_2$  (2) ${}^{28}$  with 1.10 equiv of molybdenum alkylidyne ( ${}^tBuO)_3Mo \equiv C(p\text{-OMe-C}_6H_4)$  (3) ${}^{33}$  in benzene at ambient temperature for 1 h generates [ ${}^tBuOCHO]Mo \equiv C(p\text{-OMe-C}_6H_4)({}^tBuO)$  (4) and 2 equiv of *tert*-butanol (Scheme 3). Removal of the free alcohol *in vacuo* 

Scheme 3. Metalation of the Proligand ['BuOCO]H<sub>2</sub> (2) with ('BuO)<sub>3</sub>Mo $\equiv$ C(p-OMe-C<sub>6</sub>H<sub>4</sub>) (3) to Synthesize Alkylidyne 4 as a Mixture of 4a and 4b

followed by trituration with pentane provides **4** as an amorphous yellow powder in 84% yield. A <sup>1</sup>H NMR spectrum (Figure S1) provides evidence that complex **4** exists in solution as a mixture of two stereoisomers **4a** and **4b** in a 1:1 ratio.

Evidence of the isomers comes from the presence of two singlets at 2.96 (4a) and 3.12 (4b) ppm in the  $^1\mathrm{H}$  NMR spectrum (benzene- $d_6$ ) corresponding to the OMe group on the alkylidyne. Further, the  $C_{ipso}$  proton on the central ring of the pincer ligand resonates at 8.52 (4a) and 8.33 (4b) ppm. Consistent with the presence of mirror symmetry, one singlet from the equivalent  $^t\mathrm{Bu}$  groups appears for each isomer. In the  $^{13}\mathrm{C}^{\{1}\mathrm{H}\}$  NMR spectrum, the alkylidyne  $\mathrm{C}_{\alpha}$ -atoms resonate at 301.3 and 302.4 ppm for 4a and 4b, respectively, and are consistent with analogous alkylidynes.  $^{33,34}$ 

1D selective gNOESY spectra of complex 4 in benzene- $d_6$  at 25 °C confirm the isomers are in dynamic equilibrium in solution (Figure 1). Selective inversion of the H33 and H37 protons at 6.71 ppm (4a) results in signal inversion at 6.46 ppm (4b) (Figure 1). Further, the NOE from H37 (6.71 ppm) to H12 (8.52 ppm) on complex 4a provides strong support that the central aryl ring of isomer 4a is within the same hemisphere as the phenyl ring of the alkylidyne. In contrast, the NOE from signals at H37 (6.46 ppm) to H9 and H10 (6.89 and 6.99 ppm) on complex 4b suggests the central aryl ring of isomer 4b and the alkylidyne phenyl ring are

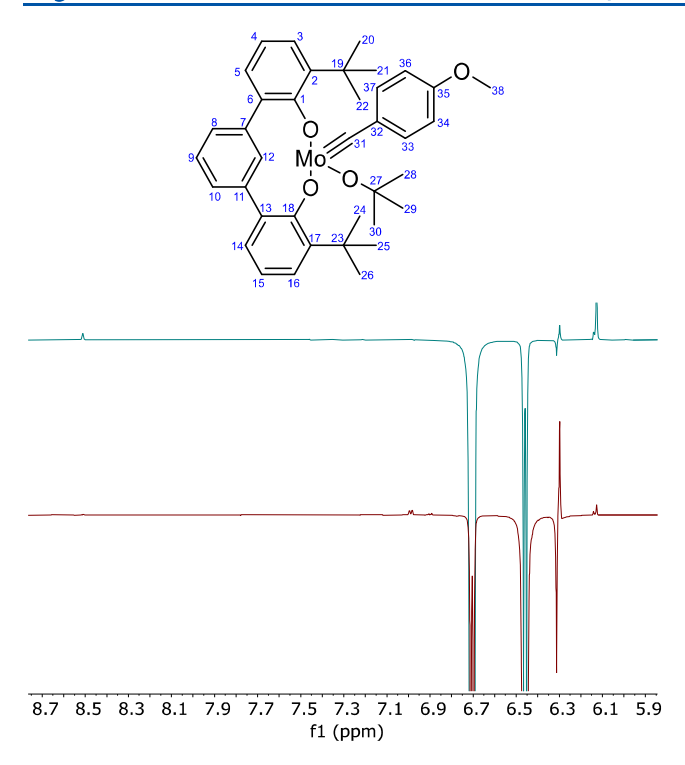


**Figure 1.** 1D gNOESY spectrum (top) irradiation of the H33 and H37 protons at 6.71 ppm results in signal inversion at 6.46 ppm (bottom) irradiation of H33 and H37 protons at 6.46 ppm results in signal inversion at 6.71 ppm in benzene- $d_6$ , 25 °C.

perpendicular to each other. Variable temperature  $^1H$  NMR spectroscopy reveals a difference in the relative free energy of the isomers. Upon cooling the solution of isomers to -60 °C in toluene- $d_8$ , NMR data reveals a ratio of 2:1 for 4a:4b, while at 70 °C, the ratio reverses to 1:2.

Isomers 4a- $d_1$  and 4b- $d_1$  are the *ipso* deuterated derivatives of 4 synthesized to probe kinetic isotope effects (KIE) during the dynamic exchange. Quenching with  $D_2O$  during the synthesis of 1 provides (1- $d_1)$ , and its subsequent use in the alkylidyne syntheses yields 4- $d_1$ . In situ  $^1H$  NMR studies of protonated and deuterated isomers 4a, 4b, 4a- $d_1$ , and 4b- $d_1$  display a KIE with  $k_H/k_D = 1.21$  (SI page S22). This value indicates a normal secondary kinetic isotope effect, suggesting that the C-H12 remains intact during isomerization.

DFT investigations at the TPSSh-D0(SMD)/cc-pVTZ//TPSSh/cc-pVDZ level of theory (see SI for details)<sup>35–50</sup> interrogate the equilibrium between **4a** and **4b**. This level of theory accurately predicts thermodynamic and kinetic data for similar complexes.<sup>51</sup> The calculations reveal the ring flip is indeed in rapid equilibrium at 25 °C with nearly thermoneutral isomers (**4a**: 0.0 kcal/mol); **4b**: -0.1 kcal/mol). Isomerization occurs without breaking bonds via a simple ring flip with a barrier (17.6 kcal/mol) low enough for quick, dynamic conversion at room temperature. Furthermore, substituting a deuterium atom at H12 perfectly matches the relative energies and barriers for their protonated counterparts (within the error of DFT), yielding a theoretical KIE of ~1.0, consistent with the experimental results.

Adding a substoichiometric amount of THF to a benzene- $d_6$  solution of **4a** and **4b** at 25 °C initiates their conversion to a single new complex with THF bound to the Mo-center (**4**<sub>THF</sub>) (Scheme 4). Indeed, DFT calculations confirm that THF stabilizes **4a** by -3.5 kcal/mol. 1D selective gNOESY spectra

### Scheme 4. Addition of THF to Isomers 4a and 4b

of the sample indicates an exchange between the  $C_{ipso}$ –H at 8.84 (4<sub>THF</sub>) and 8.56 (4a) ppm, and between the H33 and H37 protons at 6.74 (4<sub>THF</sub>) and 6.50 (4b) ppm. Further, adding an excess of THF to the solution results in complete conversion to 4<sub>THF</sub>. Signals for the coordinated THF appear at 3.55 and 1.41 ppm, each integrating to 4H. In the gHMBC NMR spectrum, complex 4<sub>THF</sub> exhibits coupling between C39, C42 carbons (3.55, 67.4 ppm) and C40, C41 carbons (1.41, 25.4 ppm), suggesting the presence of a bound THF on the Mo alkylidyne. Spectra for complex 4 do not contains signals for THF.

The NOE from 8.84 to 3.55 ppm validates the presence of bound THF. Additionally, the chemical shifts and NOEs for H33 and H37 demonstrate that  $\mathbf{4}_{\text{THF}}$  has a geometry similar to  $\mathbf{4a}$ . Complex  $\mathbf{4}_{\text{THF}}$  is also  $C_{\text{s}}$  symmetric and the alkylidyne  $C_{\alpha}$ -atom appears upfield, at 296.7 ppm, in comparison to both isomers  $\mathbf{4a}$  and  $\mathbf{4b}$ .

Conclusive evidence for the molecular structure of  $4_{THF}$  comes from an XRD experiment performed on single crystals obtained from the diffusion of pentane into a concentrated THF solution of  $4_{THF}$  at -35 °C. Figure 2 depicts the solid-

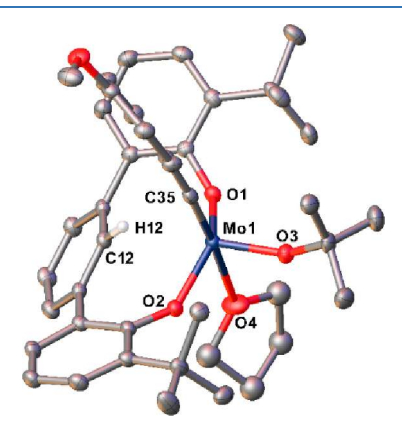


Figure 2. Molecular structure of ['BuOCHO]Mo≡C(p-OMe-C<sub>6</sub>H<sub>4</sub>)(O'Bu)(THF) (4<sub>THF</sub>). The hydrogen atoms are removed for clarity. Selected bond distances [Å]: Mo1−C35 1.757(2), Mo1−O3 1.8672(16), Mo1−O1 1.9440(15), Mo1−O2 1.9483(15), and Mo1−O4 2.4317(17). Selected bond angles [°]: ∠C35−Mo1−O3 104.63(9), ∠C35−Mo1−O1 99.56(8), ∠O3−Mo1−O1 105.47(7), ∠C35−Mo1−O2 101.43(8), ∠O3−Mo1−O2 105.58(7), ∠O1−Mo1−O2 136.35(6), ∠C35−Mo1−O4 174.38(9), ∠O3−Mo1−O4 80.90(7), ∠O1−Mo1−O4 77.78(6), and ∠O2−Mo1−O4 77.68(6).

state molecular structure of  $4_{\rm THF}$ , and the caption lists pertinent bond lengths and angles. The asymmetric unit of  $4_{\rm THF}$  consists of two chemically equivalent but crystallographically independent Mo complexes. One THF ligand displays disorder and is refined in two parts. Complex  $4_{\rm THF}$  is pseudo  $C_{\rm s}$  symmetric in the solid state and contains a formal

Mo(VI) ion in a distorted trigonal bipyramidal geometry (tbp) with an Addison parameter  $\tau_5 = 0.63$ .

The pincer ligand chelates through the phenolate donors at the equatorial sites creating an expanded  $\angle$ O1–Mo1–O2 angle of 136.35(6)°, and the *tert*-butoxide ligand occupies the remaining equatorial coordination site. The anisole alkylidyne and the THF molecule occupy the axial sites with a near-linear angle C35–Mo1–O4 of 174.38(9)° and a Mo1–C35 bond length of 1.757(2) Å. The length of the Mo $\equiv$ C alkylidyne falls within the typical range. <sup>33,34,53,54</sup> The THF ligand is *trans* to the alkylidyne ligand and exhibits a long Mo1–O4 bond length of 2.4317(17) Å.

Treating **4a** and **4b** with methylenetriphenylphosphorane  $(Ph_3P = CH_2)^{55,56}$  in  $Et_2O$  at ambient temperature for 1 h precipitates the analytically pure trianionic pincer alkylidyne salt  $\{CH_3PPh_3\}\{[{}^tBuOCO]Mo = C(p-OMe-C_6H_4)(O{}^tBu)$  (**5**) in 75% yield (Scheme 5). The reaction results in a color

# Scheme 5. Synthesis of $\{CH_3PPh_3\}\{[^tBuOCO]Mo \equiv C(p-OMe-C_6H_4)(O^tBu)$ (5)

change of the solution from yellow to red, indicating the successful removal of the Cipso-H proton. A combination of <sup>1</sup>H, <sup>13</sup>C{<sup>1</sup>H}, <sup>31</sup>P{<sup>1</sup>H}, multinuclear gHSQC, and gHMBC NMR experiments confirm the identity of 5 and permit its structural assignment. In contrast to the analogous Walkylidyne salt,<sup>57</sup> complex **5** displays poor solubility in most nonpolar solvents. In THF-d<sub>8</sub>, the lack of the C<sub>inso</sub>-H resonance confirms the identity of complex 5. Additionally, the <sup>13</sup>C{<sup>1</sup>H} NMR spectrum contains a diagnostic signal for the formation of the trianionic pincer ligand. For complex 5, the  $C_{ivso}$  resonates at 197.6 ppm (THF- $d_8$ ), which is downfieldshifted compared to the C<sub>ipso</sub> in 4a and 4b found at 122.6 and 114.7 ppm (benzene- $d_6$ ). Also, the alkylidyne  $C_{\alpha}$ -atom in complex 5 resonates at 299.6 ppm. Other structurally verified Mo and W-anionic alkylidynes<sup>34,57</sup> exhibit similar downfield  $C_{inso}$  and alkylidyne  $C_{\alpha}$ -atom resonances. In the <sup>1</sup>H NMR spectrum, a doublet ( $J_{HP} = 13.3 \text{ Hz}$ ) at 1.97 ppm is attributable to the methyl protons of the phosphonium countercation, and the corresponding phosphorus resonates at 21.3 ppm in the  $^{31}P\{^{1}H\}$  NMR spectrum. Consistent again with  $C_s$  symmetry, the <sup>1</sup>H NMR contains one singlet resonance at 1.58 ppm for the <sup>t</sup>Bu protons on the pincer ligand.

Single crystals amenable to X-ray diffraction deposit at ambient temperature by vapor diffusion of pentane into a concentrated solution of **5** in THF after 2 d. Figure 3 depicts the solid-state structure of **5**. Complex **5** is  $C_s$ -symmetric, and the molybdenum ion adopts a distorted square pyramidal geometry ( $\tau_5 = 0.18$ ),<sup>52</sup> with the Mo $\equiv$ C bond occupying the axial position. The ['BuOCO]<sup>3-</sup> trianionic pincer and the *tert*-butoxide ligands coordinate in the basal plane. The Mo(VI) ion resides 0.429 Å above the O1–C12–O2-O3 basal plane. The Mo–C<sub>ipso</sub> bond length of 2.2062(16) Å is normal compared to other trianionic pincer molybdenum complexes. <sup>28,58,59</sup> The Mo1–C31 bond length is 1.7551(17) Å,

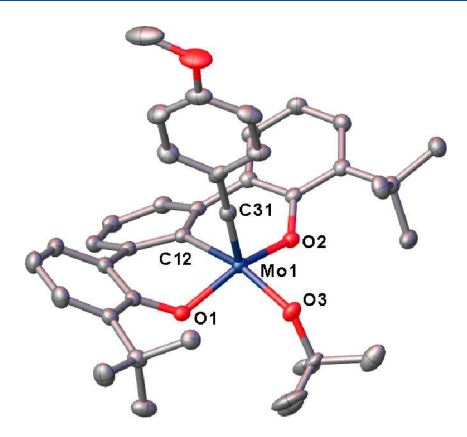


Figure 3. Molecular structure of  $\{CH_3PPh_3\}\{[^tBuOCO]Mo \equiv C(p-OMe-C_6H_4)(O^tBu)$  (5). The countercation  $[Ph_3PCH_3]^+$ , hydrogen atoms, and lattice solvent molecule (n-pentane) are removed for clarity. Selected bond distances  $[\mathring{A}]$ : Mo1−C31 1.75S1(17), Mo1−O3 1.96S7(12), Mo1−O1 1.9689(12), Mo1−O2 1.97S3(12), Mo1−C12 2.2062(16). Selected bond angles  $[^\circ]$ : ∠C31−Mo1−O3 107.8S(6), ∠C31−Mo1−O1 101.19(7), ∠O3−Mo1−O1 92.02(5), ∠C31−Mo1−O2 106.49(7), ∠O3−Mo1−O2 92.37(5), ∠O1−Mo1−O2 149.09(5), ∠C31−Mo1−C12 92.09(7), ∠O3−Mo1−C12 160.03(6), ∠O1−Mo1−C12 82.76(6), ∠O2−Mo1−C12 82.76(6).

similar to complex  $\mathbf{4}_{THF}$  and slightly shorter than the Mo $\equiv$ C bond length of 1.7676(13) Å in ['BuOCO]Mo $\equiv$ CMes-(THF)<sub>2</sub>.<sup>34</sup> The complex displays similar characteristic features to the only other crystallographically characterized anionic Walkylidyne, {CH<sub>3</sub>PPh<sub>3</sub>}{[CF<sub>3</sub>-ONO]W $\equiv$ C'Bu(O'Bu).<sup>60</sup>

Adding methyl triflate (MeOTf) to the chilled (-35 °C) anionic Mo-alkylidyne (5) solution in a 4:1 (v/v) mixture of Et<sub>2</sub>O and THF results in an immediate color change from red to dark brown. Stirring the reaction mixture for 1 h generates the neutral trianionic pincer alkylidyne [ ${}^tBuOCO$ ]Mo $\equiv C(p-OMe-C_6H_4)(THF)_2$  (6) (Scheme 6). Removing the methyl

# Scheme 6. Synthesis of [ ${}^{t}BuOCO$ ]Mo $\equiv C(p$ -OMe- $C_6H_4$ )(THF)<sub>2</sub> (6)

triphenylphosphonium triflate salt ([Ph<sub>3</sub>PCH<sub>3</sub>][OSO<sub>2</sub>CF<sub>3</sub>]) by filtration and volatiles *in vacuo* generates alkylidyne **6** as a dark brown-yellow solid in 63% yield. The <sup>1</sup>H NMR spectrum of **6** in THF- $d_8$  again exhibits resonances consistent with a  $C_s$ -symmetric complex; for instance, a single resonance appears for the pincer <sup>1</sup>Bu protons at 1.62 ppm. Most evident within the <sup>1</sup>H NMR spectrum of **6** is the presence of two broad resonances at 3.62 and 1.77 ppm for the two bound THF molecules. A downfield resonance at 316.4 ppm in the <sup>13</sup>C{<sup>1</sup>H} NMR spectrum is attributable to the Mo $\equiv$ C carbon, and a resonance at 193.1 ppm corresponds to the pincer Mo $\equiv$ C<sub>ipso</sub> carbon.

Complex 6 reacts rapidly with 5 equiv of *tert*-butylacetylene in toluene at ambient temperature to yield  $[O_2C((p\text{-OMe-}C_6H_4)C=)Mo(\eta^2\text{-CH}\equiv C^tBu)(THF)]$  (7) in quantitative isolable yields. Upon addition of the alkyne, the solution

immediately changes from dark brown-yellow to orange-yellow, suggesting the reductive migratory insertion of alkylidyne into the  $Mo-C_{ipso}$  bond (Scheme 7). Further, a  $^1H$  NMR spectrum indicates the formation of exclusively one product in the reaction mixture.

# Scheme 7. Synthesis of $[O_2C((p\text{-}OMe\text{-}C_6H_4)C=)Mo(\eta^2\text{-}CH\equiv C^tBu)(THF)]$ (7)

In benzene- $d_6$ , complex 7 exhibits a  $^1\text{H}$  NMR spectrum indicative of  $C_s$  symmetry. Two singlets attributable to the pincer and coordinated alkyne  $^t\text{Bu}$  groups resonate at 1.20 and 1.73 ppm, respectively. A downfield singlet at 10.90 ppm correlates with the proton on the  $\eta^2$ -HC $\equiv$ C $^t\text{Bu}$  moiety. In the  $^{13}\text{C}\{^1\text{H}\}$  NMR spectrum, the alkylidene carbon appears at 271.3 ppm, consistent with known pincer-supported alkylidene complexes.  $^{15-17,26,34,51,59,61,62}$  Furthermore, a resonance at 128.4 ppm corresponds to the  $C_{ipso}$  of the central pincer aryl ring, again indicating that the backbone of the ligand is not directly attached to the Mo(VI) metal center, as the  $C_{ipso}$ -Mo resonance commonly appears further downfield, around 200 ppm.  $^{34}$ 

Complex 7 is an active catalyst for the ring-expansion polymerization (REP) of phenylacetylene (PA) to give cyclic polyphenylacetylene (c-PPA) (Scheme 8). Treating a solution

# Scheme 8. Polymerization of Phenylacetylene (PA) by Complex 7 to Generate Cyclic Polyphenylacetylene (c-PPA)

of 500  $\mu$ mol phenylacetylene in 2 mL toluene with 7 for 1, 2, 5, 10, and 24 h at ambient temperature produces c-PPA (Table 1). Polymerization at 1 h yields a polymer too small for GPC. The polymerization continues up to 24 h, and the yield increases with reaction time. The  $M_{\rm n}$  ranges between 5600 and 39000 g/mol with the largest polymers produced in 10 h. Other reported Mo-alkylidynes produced PPA with  $M_{\rm n}$  ranging from 1500 to 8000 g/mol.  $^{63}$ 

Evidence for a cyclic topology comes from various measurements that probe the hydrodynamic volume of the polymers. The commercially available complex acetylacetonato(1,5-cyclooctadiene) rhodium(I) (8)<sup>64</sup> is an active catalyst for linear polyphenylacetylene (*l*-PPA) synthesis. Mixing a solution of complex 8 in THF with phenylacetylene for 3 h provides the *l*-PPA.<sup>65</sup> Figure 4 depicts

Table 1. Polymerization of Phenylacetylene<sup>a</sup> by Complex 7 with Different Reaction Times

reaction time (h)	yield (%)	$M_{\rm n}^{\ b}$ (g/mol)	$M_{\rm w}/M_{\rm n}^{}$
1	15	N/A	N/A
2	30	5600	2.18
5	47	36000	2.33
10	63	39000	2.27
24	76	31000	2.80

<sup>a</sup>The appropriate amount of catalyst solution in toluene (10 mg/mL) is added to phenylacetylene dissolved in toluene and stirred at ambient temperature for different reaction times. <sup>b</sup>Determined by size-exclusion chromatography (SEC) using THF as a mobile phase at 35 °C equipped with multiangle light scattering (MALS) detection.

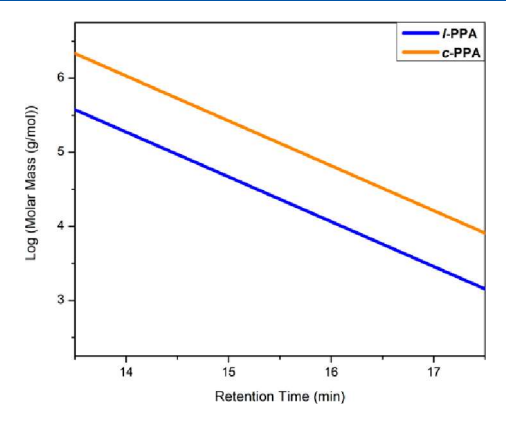


Figure 4. Log of molar mass versus retention time for polyphenylacetylene synthesized by complex 7 (cyclic) and by complex 8 (linear).

a plot of log of molar mass versus retention time. Cyclic polymers with the same molar mass elute later than their linear counterparts because of their smaller hydrodynamic volume. Indeed, Figure 4 reveals that cyclic structures elute later than linear ones over a broad range of molar mass.

Confirmation of the cyclic topology also comes from the demonstration of lower intrinsic viscosities of cyclic versus linear PPA samples ( $[\eta]_{\text{cyclic}} < [\eta]_{\text{linear}}$ ) via a Mark–Houwink–Sakurada (MHS) plot ( $[\eta]$  is the intrinsic viscosity and M is the viscosity-average molar mass) (Figure 5). The experimental ratio  $[\eta]_{\text{cyclic}}/[\eta]_{\text{linear}}$  of 0.43  $\pm$  0.12 over a range of molecular weights is within the limits expected for the topological difference. Under  $\theta$  conditions (a = 0.5), the

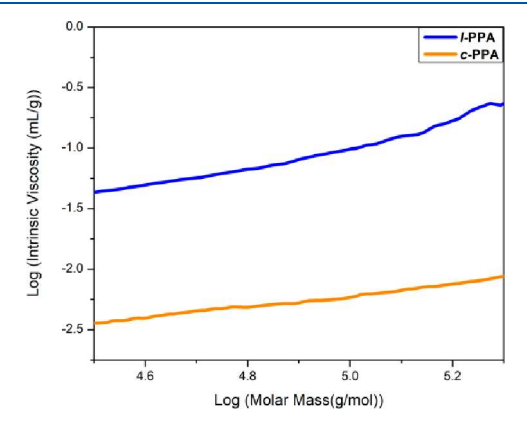
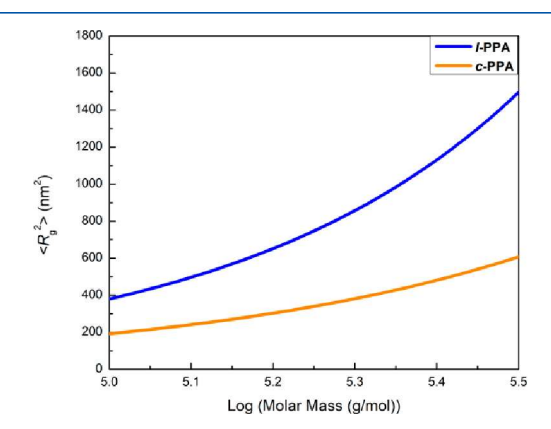


Figure 5. Log of [n] versus log of molar mass for polyphenylacetylene synthesized by complex 7 (cyclic) and by complex 8 (linear).

predicted range of ratios are between  $0.65^{66,67}$  and  $0.58 \pm 0.01.^{68}$  Depending on the molecular weight<sup>69,70</sup> and the polymer–solvent system,<sup>71,72</sup> experimental results range from  $\sim 0.4$  to  $\sim 0.8.^{10,69,71}$  The polymers synthesized with complexes 7 and 8 depict MHS parameter a values of 0.485 and 0.927, indicating the different behaviors of polymers in solution.

Figure 6 depicts the root-mean-square radius  $(\langle R_g^2 \rangle)$  versus the log of molecular weight of *l*-PPA versus *c*-PPA. The



**Figure 6.** Plot of root-mean-square radius  $(\langle R_g^2 \rangle)$  versus log of molar mass for polyphenylacetylene synthesized by complex 7 (cyclic) and by complex 8 (linear).

molecular weight of the linear analogue increases at a greater rate than the more compact cyclic polymers. As the molecular weight grows, the linear analogue will increase in size more rapidly than the more compact cyclic polymer. The cyclic and linear polyphenylacetylene demonstrate a  $\langle R_{\rm g}^{\ 2} \rangle_{\rm cyclic}/\langle R_{\rm g}^{\ 2} \rangle_{\rm linear}$  ratio of 0.455  $\pm$  0.05, which is within the experimental error of the theoretical value of 0.5.  $^{73,74}$ 

A safer, less expensive, and scalable synthesis for the trianionic pincer ligand precursor [\*BuOCO]Me<sub>2</sub> (1) is now available. The new cyclic polymer catalyst  $[O_2C((p-OMe-P))]$  $C_6H_4)C = Mo(\eta^2-CH \equiv C^tBu)(THF)$  7 was synthesized. Using this new approach, it is possible to functionalize the  $C_{inso}$  of the pincer carbon. Placing an iodide in that position is plausible from literature precedent. In this work, deuterium was substituted by quenching with D2O. The isomers [ ${}^{t}BuOCHO$ ]Mo $\equiv C(p-OMe-C_6H_4)(O{}^{t}Bu)$  (4a and 4b) are in dynamic equilibrium where the pincer central aryl ring flips rapidly at ambient temperatures in solution with a modest KIE. Complex 7 adds to the list of REP catalysts for the synthesis of cyclic polyphenylacetylene (c-PPA). However, the activity pales in comparison to the corresponding W-derivatives. 26,57,61,75 This fact may be important in elucidating the mechanism of the polymerization, which is still under investigation in our laboratories.

# ASSOCIATED CONTENT

## Supporting Information

The Supporting Information is available free of charge at https://pubs.acs.org/doi/10.1021/acs.organomet.3c00060.

Full experimental procedures, NMR spectra, X-ray crystallographic and GC/EI-MS data (PDF)

### **Accession Codes**

CCDC 2226075-2226077 contain the supplementary crystallographic data for this paper. These data can be obtained free of charge via www.ccdc.cam.ac.uk/data\_request/cif, or by

emailing data\_request@ccdc.cam.ac.uk, or by contacting The Cambridge Crystallographic Data Centre, 12 Union Road, Cambridge CB2 1EZ, UK; fax: +44 1223 336033.

### AUTHOR INFORMATION

### **Corresponding Author**

Adam S. Veige — Department of Chemistry, Center for Catalysis, University of Florida, Gainesville, Florida 32611, United States; orcid.org/0000-0002-7020-9251; Email: veige@chem.ufl.edu

#### **Authors**

Vineet K. Jakhar – Department of Chemistry, Center for Catalysis, University of Florida, Gainesville, Florida 32611, United States

**Yu-Hsuan Shen** — Department of Chemistry, Center for Catalysis, University of Florida, Gainesville, Florida 32611, United States; Occid.org/0000-0003-0976-4034

Sung-Min Hyun — Department of Chemistry, Center for Catalysis, University of Florida, Gainesville, Florida 32611, United States

Alec M. Esper — Department of Chemistry, Center for Catalysis, University of Florida, Gainesville, Florida 32611, United States

**Ion Ghiviriga** — Department of Chemistry, Center for Catalysis, University of Florida, Gainesville, Florida 32611, United States; <sup>⑤</sup> orcid.org/0000-0001-5812-5170

Khalil A. Abboud – Department of Chemistry, Center for Catalysis, University of Florida, Gainesville, Florida 32611, United States

Daniel W. Lester – Polymer Characterization Research Technology Platform, University of Warwick, Coventry CV4 7AL, United Kingdom

Complete contact information is available at: https://pubs.acs.org/10.1021/acs.organomet.3c00060

#### Notes

The authors declare no competing financial interest.

# ■ ACKNOWLEDGMENTS

This material is based upon work supported by the National Science Foundation CHE-2154377 (A.S.V.). The GC/EI-MS instrument is funded by NIH S10 OD021758-01A1. K.A.A. acknowledges the NSF (CHE-1828064) and UF for the purchase of X-ray equipment.

### REFERENCES

- (1) Xia, Y.; Boydston, A. J.; Yao, Y.; Kornfield, J. A.; Gorodetskaya, I. A.; Spiess, H. W.; Grubbs, R. H. Ring-Expansion Metathesis Polymerization: Catalyst-Dependent Polymerization Profiles. *J. Am. Chem. Soc.* **2009**, *131* (7), 2670–2677.
- (2) Boydston, A. J.; Xia, Y.; Kornfield, J. A.; Gorodetskaya, I. A.; Grubbs, R. H. Cyclic Ruthenium-Alkylidene Catalysts for Ring-Expansion Metathesis Polymerization. *J. Am. Chem. Soc.* **2008**, *130* (38), 12775–12782.
- (3) Nasongkla, N.; Chen, B.; Macaraeg, N.; Fox, M. E.; Fréchet, J. M. J.; Szoka, F. C. Dependence of Pharmacokinetics and Biodistribution on Polymer Architecture: Effect of Cyclic versus Linear Polymers. J. Am. Chem. Soc. 2009, 131 (11), 3842–3843.
- (4) Chen, B.; Jerger, K.; Fréchet, J. M. J.; Szoka, F. C. The Influence of Polymer Topology on Pharmacokinetics: Differences between Cyclic and Linear PEGylated Poly(Acrylic Acid) Comb Polymers. J. Controlled Release 2009, 140 (3), 203–209.

- (5) Golba, B.; Benetti, E. M.; de Geest, B. G. Biomaterials Applications of Cyclic Polymers. *Biomaterials* **2021**, *267*, 120468.
- (6) Patel, A.; Cosgrove, T.; Semlyen, J. A. Studies of Cyclic and Linear Poly(Dimethylsiloxanes): 30. Adsorption Studies on Silica in Solution. *Polymer (Guildf)* **1991**, 32 (7), 1313–1317.
- (7) Verbraeken, B.; Hoogenboom, R. Cyclic Polymers: From Scientific Curiosity to Advanced Materials for Gene Delivery and Surface Modification. *Angew. Chem., Int. Ed.* **2017**, *56* (25), 7034–7036.
- (8) Morgese, G.; Trachsel, L.; Romio, M.; Divandari, M.; Ramakrishna, S. N.; Benetti, E. M. Topological Polymer Chemistry Enters Surface Science: Linear versus Cyclic Polymer Brushes. *Angew. Chem., Int. Ed.* **2016**, *55* (50), 15583–15588.
- (9) Wang, L.; Xu, L.; Liu, B.; Shi, T.; Jiang, S.; An, L. The Influence of Polymer Architectures on the Dewetting Behavior of Thin Polymer Films: From Linear Chains to Ring Chains. *Soft Matter* **2017**, *13* (17), 3091–3098.
- (10) Jeong, Y.; Jin, Y.; Chang, T.; Uhlik, F.; Roovers, J. Intrinsic Viscosity of Cyclic Polystyrene. *Macromolecules* **2017**, *50* (19), 7770–7776.
- (11) Honda, S.; Yamamoto, T.; Tezuka, Y. Topology-Directed Control on Thermal Stability: Micelles Formed from Linear and Cyclized Amphiphilic Block Copolymers. *J. Am. Chem. Soc.* **2010**, *132* (30), 10251–10253.
- (12) Orrah, D. J.; Semlyen, J. A.; Ross-Murphy, S. B. Studies of Cyclic and Linear Poly(Dimethylsiloxanes): 28. Viscosities and Densities of Ring and Chain Poly(Dimethylsiloxane) Blends. *Polymer (Guildf)* 1988, 29 (8), 1455–1458.
- (13) Bannister, D. J.; Semlyen, J. A. Studies of Cyclic and Linear Poly(Dimethyl Siloxanes): 6. Effect of Heat. *Polymer (Guildf)* **1981**, 22 (3), 377–381.
- (14) Mandal, U.; Ghiviriga, I.; Abboud, K. A.; Lester, D. W.; Veige, A. S. Double Tethered Metallacyclobutane Catalyst for Cyclic Polymer Synthesis. *J. Am. Chem. Soc.* **2021**, *143* (41), 17276–17283.
- (15) Gonsales, S. A.; Kubo, T.; Flint, M. K.; Abboud, K. A.; Sumerlin, B. S.; Veige, A. S. Highly Tactic Cyclic Polynorbornene: Stereoselective Ring Expansion Metathesis Polymerization of Norbornene Catalyzed by a New Tethered Tungsten-Alkylidene Catalyst. J. Am. Chem. Soc. 2016, 138 (15), 4996–4999.
- (16) Nadif, S. S.; Kubo, T.; Gonsales, S. A.; VenkatRamani, S.; Ghiviriga, I.; Sumerlin, B. S.; Veige, A. S. Introducing "Ynene" Metathesis: Ring-Expansion Metathesis Polymerization Leads to Highly Cis and Syndiotactic Cyclic Polymers of Norbornene. *J. Am. Chem. Soc.* **2016**, *138* (20), 6408–6411.
- (17) Jakhar, V.; Pal, D.; Ghiviriga, I.; Abboud, K. A.; Lester, D. W.; Sumerlin, B. S.; Veige, A. S. Tethered Tungsten-Alkylidenes for the Synthesis of Cyclic Polynorbornene via Ring Expansion Metathesis: Unprecedented Stereoselectivity and Trapping of Key Catalytic Intermediates. J. Am. Chem. Soc. 2021, 143 (2), 1235–1246.
- (18) Edwards, J. P.; Wolf, W. J.; Grubbs, R. H. The Synthesis of Cyclic Polymers by Olefin Metathesis: Achievements and Challenges. J. Polym. Sci. A Polym. Chem. 2019, 57 (3), 228–242.
- (19) Wang, T.-W.; Huang, P.-R.; Chow, J. L.; Kaminsky, W.; Golder, M. R. A Cyclic Ruthenium Benzylidene Initiator Platform Enhances Reactivity for Ring-Expansion Metathesis Polymerization. *J. Am. Chem. Soc.* **2021**, *143* (19), 7314–7319.
- (20) Yoon, K.-Y.; Noh, J.; Gan, Q.; Edwards, J. P.; Tuba, R.; Choi, T.-L.; Grubbs, R. H. Scalable and Continuous Access to Pure Cyclic Polymers Enabled by 'Quarantined' Heterogeneous Catalysts. *Nat. Chem.* **2022**, *14* (11), 1242–1248.
- (21) Morrison, C. M.; Golder, M. R. Ring-Expansion Metathesis Polymerization Initiator Design for the Synthesis of Cyclic Polymers. *Synlett* **2022**, 33 (08), 699–704.
- (22) Bielawski, C. W.; Benitez, D.; Grubbs, R. H. Synthesis of Cyclic Polybutadiene via Ring-Opening Metathesis Polymerization: The Importance of Removing Trace Linear Contaminants. *J. Am. Chem. Soc.* 2003, 125 (28), 8424–8425.
- (23) Zhang, K.; Lackey, M. A.; Wu, Y.; Tew, G. N. Universal Cyclic Polymer Templates. J. Am. Chem. Soc. **2011**, 133 (18), 6906–6909.

- (24) Xia, Y.; Boydston, A. J.; Grubbs, R. H. Synthesis and Direct Imaging of Ultrahigh Molecular Weight Cyclic Brush Polymers. *Angew. Chem., Int. Ed.* **2011**, *50* (26), 5882–5885.
- (25) Zhang, K.; Lackey, M. A.; Cui, J.; Tew, G. N. Gels Based on Cyclic Polymers. J. Am. Chem. Soc. **2011**, 133 (11), 4140–4148.
- (26) Roland, C. D.; Li, H.; Abboud, K. A.; Wagener, K. B.; Veige, A. S. Cyclic Polymers from Alkynes. *Nat. Chem.* **2016**, 8 (8), 791–796.
- (27) Agapie, T.; Bercaw, J. E. Cyclometalated Tantalum Diphenolate Pincer Complexes: Intramolecular  $C-H/M-CH_3$   $\sigma$ -Bond Metathesis May Be Faster than  $O-H/M-CH_3$  Protonolysis. *Organometallics* **2007**, 26 (12), 2957–2959.
- (28) Sarkar, S.; Carlson, A. R.; Veige, M. K.; Falkowski, J. M.; Abboud, K. A.; Veige, A. S. Synthesis, Characterization, and Reactivity of a d<sup>2</sup>, Mo(IV) Complex Supported by a New OCO—Trianionic Pincer Ligand. *J. Am. Chem. Soc.* **2008**, *130* (4), 1116–1117.
- (29) Grewal, R. S.; Hart, H.; Vinod, T. K. Oxacyclophanes Based on a m-Terphenyl Framework. J. Org. Chem. 1992, 57 (9), 2721–2726.
- (30) Saednya, A.; Hart, H. Two Efficient Routes to *m*-Terphenyls from 1,3-Dichlorobenzenes. *Synthesis* (Stuttg) **1996**, 1996 (12), 1455–1458.
- (31) Ovaska, T. v.; Snieckus, V.; Nolte, B. *n*-Butyllithium. *Encyclopedia of Reagents for Organic Synthesis* **2009**, DOI: 10.1002/047084289X.rb395.pub2.
- (32) Bailey, W. F.; Wachter-Jurcsak, N. t-Butyllithium. Encyclopedia of Reagents for Organic Synthesis 2009, DOI: 10.1002/047084289X.rb396.pub2.
- (33) Hillenbrand, J.; Leutzsch, M.; Fürstner, A. Molybdenum Alkylidyne Complexes with Tripodal Silanolate Ligands: The Next Generation of Alkyne Metathesis Catalysts. *Angew. Chem., Int. Ed.* **2019**, 58 (44), 15690–15696.
- (34) Roland, C. D.; VenkatRamani, S.; Jakhar, V. K.; Ghiviriga, I.; Abboud, K. A.; Veige, A. S. Synthesis and Characterization of a Molybdenum Alkylidyne Supported by a Trianionic OCO<sup>3-</sup> Pincer Ligand. *Organometallics* **2018**, *37* (23), 4500–4505.
- (35) Frisch, M. J.; Trucks, G. W.; Schlegel, H. B.; Scuseria, G. E.; Robb, M. A.; Cheeseman, J. R.; Scalmani, G.; Barone, V.; Petersson, G. A.; Nakatsuji, H.; Li, X.; Caricato, M.; Marenich, A. V.; Bloino, J.; Janesko, B. G.; Gomperts, R.; Mennucci, B.; Hratchian, H. P.; Ortiz, J. V.; Izmaylov, A. F.; Sonnenberg, J. L.; Williams; Ding, F.; Lipparini, F.; Egidi, F.; Goings, J.; Peng, B.; Petrone, A.; Henderson, T.; Ranasinghe, D.; Zakrzewski, V. G.; Gao, J.; Rega, N.; Zheng, G.; Liang, W.; Hada, M.; Ehara, M.; Toyota, K.; Fukuda, R.; Hasegawa, J.; Ishida, M.; Nakajima, T.; Honda, Y.; Kitao, O.; Nakai, H.; Vreven, T.; Throssell, K.; Montgomery, J. A., Jr.; Peralta, J. E.; Ogliaro, F.; Bearpark, M. J.; Heyd, J. J.; Brothers, E. N.; Kudin, K. N.; Staroverov, V. N.; Keith, T. A.; Kobayashi, R.; Normand, J.; Raghavachari, K.; Rendell, A. P.; Burant, J. C.; Iyengar, S. S.; Tomasi, J.; Cossi, M.; Millam, J. M.; Klene, M.; Adamo, C.; Cammi, R.; Ochterski, J. W.; Martin, R. L.; Morokuma, K.; Farkas, O.; Foresman, J. B.; Fox, D. J. Gaussian 16, Revision C.01; Gaussian Inc.: Wallingford, CT, 2016.
- (36) Dennington, R.; Keith, T. A.; Millam, J. M. GaussView, Version 6.0.16; Semichem Inc.: Shawnee Mission, KS, 2016.
- (37) Tao, J.; Perdew, J. P.; Staroverov, V. N.; Scuseria, G. E. Climbing the Density Functional Ladder: Nonempirical Meta—Generalized Gradient Approximation Designed for Molecules and Solids. *Phys. Rev. Lett.* **2003**, *91* (14), 146401.
- (38) Balabanov, N. B.; Peterson, K. A. Systematically Convergent Basis Sets for Transition Metals. I. All-Electron Correlation Consistent Basis Sets for the 3d Elements Sc–Zn. J. Chem. Phys. 2005, 123 (6), 064107.
- (39) Balabanov, N. B.; Peterson, K. A. Basis Set Limit Electronic Excitation Energies, Ionization Potentials, and Electron Affinities for the 3d Transition Metal Atoms: Coupled Cluster and Multireference Methods. J. Chem. Phys. 2006, 125 (7), 074110.
- (40) Schuchardt, K. L.; Didier, B. T.; Elsethagen, T.; Sun, L.; Gurumoorthi, V.; Chase, J.; Li, J.; Windus, T. L. Basis Set Exchange: A Community Database for Computational Sciences. *J. Chem. Inf. Model.* **2007**, 47 (3), 1045–1052.

- (41) Baerends, E. J.; Ellis, D. E.; Ros, P. Self-Consistent Molecular Hartree—Fock—Slater Calculations I. The Computational Procedure. *Chem. Phys.* **1973**, 2 (1), 41–51.
- (42) Whitten, J. L. Coulombic Potential Energy Integrals and Approximations. J. Chem. Phys. 1973, 58 (10), 4496–4501.
- (43) Feyereisen, M.; Fitzgerald, G.; Komornicki, A. Use of Approximate Integrals in Ab Initio Theory. An Application in MP2 Energy Calculations. *Chem. Phys. Lett.* **1993**, 208 (5–6), 359–363.
- (44) Vahtras, O.; Almlöf, J.; Feyereisen, M. W. Integral Approximations for LCAO-SCF Calculations. *Chem. Phys. Lett.* **1993**, 213 (5–6), 514–518.
- (45) Hratchian, H. P.; Schlegel, H. B. Using Hessian Updating To Increase the Efficiency of a Hessian Based Predictor-Corrector Reaction Path Following Method. *J. Chem. Theory Comput.* **2005**, *1* (1), 61–69.
- (46) Marenich, A. v.; Cramer, C. J.; Truhlar, D. G. Universal Solvation Model Based on Solute Electron Density and on a Continuum Model of the Solvent Defined by the Bulk Dielectric Constant and Atomic Surface Tensions. *J. Phys. Chem. B* **2009**, *113* (18), 6378–6396.
- (47) Grimme, S. Density Functional Theory with London Dispersion Corrections. Wiley Interdiscip. Rev. Comput. Mol.Sci. 2011, 1 (2), 211–228.
- (48) Tobisch, S.; Ziegler, T. Catalytic Oligomerization of Ethylene to Higher Linear  $\alpha$ -Olefins Promoted by the Cationic Group 4  $[(\eta^5-Cp-(CMe_2-Bridge)-Ph)M^{II}(Ethylene)_2]^+$  (M=Ti, Zr, Hf) Active Catalysts: A Density Functional Investigation of the Influence of the Metal on the Catalytic Activity and Selectivity. *J. Am. Chem. Soc.* **2004**, 126 (29), 9059–9071.
- (49) Zaccaria, F.; Ehm, C.; Budzelaar, P. H. M.; Busico, V. Accurate Prediction of Copolymerization Statistics in Molecular Olefin Polymerization Catalysis: The Role of Entropic, Electronic, and Steric Effects in Catalyst Comonomer Affinity. ACS Catal. 2017, 7 (2), 1512–1519.
- (50) Zaccaria, F.; Cipullo, R.; Budzelaar, P. H. M.; Busico, V.; Ehm, C. Backbone Rearrangement during Olefin Capture as the Rate Limiting Step in Molecular Olefin Polymerization Catalysis and Its Effect on Comonomer Affinity. *J. Polym. Sci. A Polym. Chem.* **2017**, 55 (17), 2807–2814.
- (51) Jakhar, V. K.; Esper, A. M.; Ghiviriga, I.; Abboud, K. A.; Ehm, C.; Veige, A. S. Isolation of an Elusive Phosphametallacyclobutadiene and Its Role in Reversible Carbon—Carbon Bond Cleavage. *Angew. Chem., Int. Ed.* **2022**, *61* (30), No. e202203073.
- (52) Addison, A. W.; Rao, T. N.; Reedijk, J.; van Rijn, J.; Verschoor, G. C. Synthesis, Structure, and Spectroscopic Properties of Copper(II) Compounds Containing Nitrogen—Sulphur Donor Ligands; the Crystal and Molecular Structure of Aqua[1,7-Bis(N-Methylbenzimidazol-2'-Yl)-2,6-Dithiaheptane]Copper(II) Perchlorate. *J. Chem. Soc., Dalton Trans.* 1984, No. 7, 1349—1356.
- (53) Heppekausen, J.; Stade, R.; Kondoh, A.; Seidel, G.; Goddard, R.; Fürstner, A. Optimized Synthesis, Structural Investigations, Ligand Tuning and Synthetic Evaluation of Silyloxy-Based Alkyne Metathesis Catalysts. *Chem. Eur. J.* **2012**, *18* (33), 10281–10299.
- (54) Koy, M.; Elser, I.; Meisner, J.; Frey, W.; Wurst, K.; Kästner, J.; Buchmeiser, M. R. High Oxidation State Molybdenum *N* -Heterocyclic Carbene Alkylidyne Complexes: Synthesis, Mechanistic Studies, and Reactivity. *Chem. Eur. J.* **2017**, *23* (61), 15484–15490.
- (55) Bestmann, H. J.; Stransky, W.; Vostrowsky, O. Reaktionen Mit Phosphinalkylenen, XXXIII. Darstellung Lithiumsalzfreier Ylidlösungen Mit Natrium-bis(Trimethylsilyl)amid Als Base. *Chem. Ber.* **1976**, 109 (5), 1694–1700.
- (56) Tonzetich, Z. J.; Schrock, R. R.; Müller, P. Reaction of Phosphoranes with  $Mo(N-2,6-i-Pr_2C_6H_3)(CHCMe_3)[OCMe-(CF_3)_2]_2$ : Synthesis and Reactivity of an Anionic Imido Alkylidyne Complex. *Organometallics* **2006**, 25 (18), 4301–4306.
- (57) Sarkar, S.; McGowan, K. P.; Kuppuswamy, S.; Ghiviriga, I.; Abboud, K. A.; Veige, A. S. An OCO<sup>3-</sup> Trianionic Pincer Tungsten(VI) Alkylidyne: Rational Design of a Highly Active Alkyne

- Polymerization Catalyst. J. Am. Chem. Soc. 2012, 134 (10), 4509-4512
- (58) Sarkar, S.; Abboud, K. A.; Veige, A. S. Addition of Mild Electrophiles to a Mo≡N Triple Bond and Nitrile Synthesis via Metal-Mediated N-Atom Transfer to Acid Chlorides. *J. Am. Chem. Soc.* **2008**, *130* (48), 16128−16129.
- (59) Jan, M. T.; Sarkar, S.; Kuppuswamy, S.; Ghiviriga, I.; Abboud, K. A.; Veige, A. S. Synthesis and Characterization of a Trianionic Pincer Supported Mo-Alkylidene Anion and Alkyne Insertion into a Mo(IV)- $C_{pincer}$  Bond to Form Metallocyclopropene( $\eta^2$ -Vinyl) Complexes. *J. Organomet. Chem.* **2011**, *696* (25), 4079–4089.
- (60) O'Reilly, M. E.; Nadif, S. S.; Ghiviriga, I.; Abboud, K. A.; Veige, A. S. Synthesis and Characterization of Tungsten Alkylidene and Alkylidyne Complexes Supported by a New Pyrrolide-Centered Trianionic ONO<sup>3</sup> Pincer-Type Ligand. *Organometallics* **2014**, *33* (4), 836–839.
- (61) McGowan, K. P.; O'Reilly, M. E.; Ghiviriga, I.; Abboud, K. A.; Veige, A. S. Compelling Mechanistic Data and Identification of the Active Species in Tungsten-Catalyzed Alkyne Polymerizations: Conversion of a Trianionic Pincer into a New Tetraanionic Pincer-Type Ligand. *Chem. Sci.* **2013**, *4* (3), 1145.
- (62) Roland, C. D.; Zhang, T.; VenkatRamani, S.; Ghiviriga, I.; Veige, A. S. A Catalytically Relevant Intermediate in the Synthesis of Cyclic Polymers from Alkynes. *Chem. Commun.* **2019**, *55* (91), 13697–13700.
- (63) Ehrhorn, H.; Bockfeld, D.; Freytag, M.; Bannenberg, T.; Kefalidis, C. E.; Maron, L.; Tamm, M. Studies on Molybdena- and Tungstenacyclobutadiene Complexes Supported by Fluoroalkoxy Ligands as Intermediates of Alkyne Metathesis. *Organometallics* **2019**, 38 (7), 1627–1639.
- (64) Trhlíková, O.; Zedník, J.; Balcar, H.; Brus, J.; Sedláček, J. [Rh(Cycloolefin)(Acac)] Complexes as Catalysts of Polymerization of Aryl- and Alkylacetylenes: Influence of Cycloolefin Ligand and Reaction Conditions. J. Mol. Catal. A Chem. 2013, 378, 57–66.
- (65) Pal, D.; Miao, Z.; Garrison, J. B.; Veige, A. S.; Sumerlin, B. S. Ultra-High-Molecular-Weight Macrocyclic Bottlebrushes via Post-Polymerization Modification of a Cyclic Polymer. *Macromolecules* **2020**, 53 (22), 9717–9724.
- (66) Bloomfield, V.; Zimm, B. H. Viscosity, Sedimentation, et Cetera, of Ring- and Straight-Chain Polymers in Dilute Solution. *J. Chem. Phys.* **1966**, 44 (1), 315–323.
- (67) Fukatsu, M.; Kurata, M. Hydrodynamic Properties of Flexible-Ring Macromolecules. J. Chem. Phys. 1966, 44 (12), 4539–4545.
- (68) Rubio, A. M.; Freire, J. J.; Bishop, M.; Clarke, J. H. R. THETA State, Transition Curves, and Conformational Properties of Cyclic Chains. *Macromolecules* 1995, 28 (7), 2240–2246.
- (69) Roovers, J. Dilute-Solution Properties of Ring Polystyrenes. J. Polym. Sci. Polym. Phys. Ed. 1985, 23 (6), 1117–1126.
- (70) Geiser, D.; Höcker, H. Synthesis and Investigation of Macrocyclic Polystyrene. *Macromolecules* 1980, 13 (3), 653–656.
- (71) McKenna, G. B.; Hadziioannou, G.; Lutz, P.; Hild, G.; Strazielle, C.; Straupe, C.; Rempp, P.; Kovacs, A. J. Dilute Solution Characterization of Cyclic Polystyrene Molecules and Their Zero-Shear Viscosity in the Melt. *Macromolecules* 1987, 20 (3), 498–512.
- (72) Lutz, P.; McKenna, G. B.; Rempp, P.; Strazielle, C. Solution Properties of Ring-Shaped Polystyrenes. *Makromol. Chem., Rapid Commun.* **1986**, 7 (9), 599–605.
- (73) Zimm, B. H.; Stockmayer, W. H. The Dimensions of Chain Molecules Containing Branches and Rings. *J. Chem. Phys.* **1949**, *17* (12), 1301–1314.
- (74) Semlyen, J. A. Cyclic Polymers; Kluwer Academic Publishers: New York, 2000.
- (75) Miao, Z.; Pal, D.; Niu, W.; Kubo, T.; Sumerlin, B. S.; Veige, A. S. Cyclic Poly(4-Methyl-1-Pentene): Efficient Catalytic Synthesis of a Transparent Cyclic Polymer. *Macromolecules* **2020**, *53* (18), 7774–7782.